



## **A 3D PANEL CODE FOR WAVE DRAG CALCULATIONS PART II: THE UPWIND TECHNIQUE**

**by M. Storti, J. Delia, S. Idelsohn**

*Grupo de Tecnología Mecánica del INTEC*

*Universidad Nacional del Litoral and CONICET*

*Güemes 3450, 3000, Santa Fe, Argentina*

*e-mail: mstorti@galileo.unl.edu.ar, <http://venus.unl.edu.ar/gtm-eng.html>*

### **SUMMARY**

We present a 3D BEM/panel code to compute potential flows about ship-forms with linearized free-surface conditions in order to compute the wave drag. Details of the 3D panel discretization and numerical results, will be given in a companion paper [1], so that this one deals with those aspects related to the implementation of the upwind technique in order to capture the "physical" admissible solutions, i.e. those ones satisfying an appropriated radiation boundary condition at infinity downstream.

The basic governing equations of potential flow with free surface are the Laplace equation for the velocity potential with appropriated boundary conditions, and the free surface condition, which is based on the Bernoulli equation and relates the surface elevation with the local absolute value of velocity. However, this problem is ill-posed in the sense that allows multiple solutions, associated with the existence of a system of trailing gravity waves. In real life, this wave system originates in the ship and propagates to infinity downstream. In 2D situations the trailing waves propagates to infinity downstream without damping, whereas in 3D situations the amplitude of the wave pattern decreases due to the spreading in the transversal direction, but keeping constant some quadratic norm of the transverse profile, associated to the wave-drag. The expenditure of energy in creating this wave pattern is at the cause of the wave drag. The set of governing equations, as described so far, allows solutions with trailing waves propagating in both (upstream and downstream) directions. Solutions with upstream propagating trailing waves should be considered non-physical and, consequently, discarded. This is done by means of the addition of an "upwind" or "artificial viscosity" term. Once this term is added, the unicity of the solution for the problem is recovered. In this paper we discuss the theoretical and practical aspects of the implementation of such term.

**Key words:** 3D BEM, potential flows, wave drag, ship forms, free surface, upwind technique, trailing gravity waves.

### **POTENTIAL FORMULATION FOR FREE SURFACE PROBLEMS**

Consider a rigid body at a constant speed in a fluid media occupying the region  $z < 0$  (see figure 1). The trajectory of the body follows a line parallel to the  $x$  coordinate, and it is such that the body is partially or totally submerged in the fluid. As the speed of the body is increased the pressure field produced by the flow perturbs the free surface and a "wave pattern" is produced. Even for inviscid flow, some energy is dispensed by the body in order to maintain this pattern, and this is

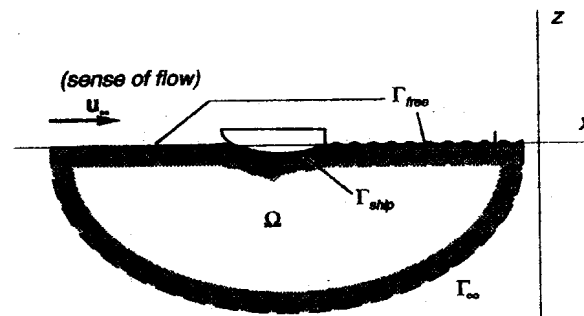


Fig 1: Problem description

possible only if a drag force acts on the body. This is called the "wave drag" and is one of the components of the drag that persist even for a negligible viscosity, like the form and shock-wave drag components. The main application is in ship hydrodynamics, and it can be seen that for very large ships, wave-drag and form-drag are the main components of drag.

Suppose that, due to the usual mechanisms of dissipation a steady state solution for the wave pattern is found. The velocity field is then governed by the following set of equations:

$$\left. \begin{aligned} \mathbf{u} &= \nabla \Phi \\ \Delta \Phi &= 0 \end{aligned} \right\} \text{ in } \Omega \quad (1)$$

where  $\mathbf{u}$  is the velocity of the fluid and  $\Phi(x, y, z)$  the total potential. The "kinematic boundary conditions" are simply the slip condition at the free surface  $\Gamma_{free}$  and on that part  $\Gamma_{ship}$  of the ship hull which is in contact with the liquid, and an equivalent condition at the infinite boundary  $\Gamma_{\infty}$ :

$$\left. \begin{aligned} \frac{\partial \Phi}{\partial n} &= 0 \text{ in } \Gamma_{free} + \Gamma_{ship} \\ \frac{\partial \Phi}{\partial n} &= \mathbf{u}_{\infty} \cdot \hat{\mathbf{n}} \text{ in } \Gamma_{\infty} \end{aligned} \right\} \quad (2)$$

This system of equations is enough if the position of the free surface is known a priori. As this is not the case, we have to add a condition, in order to adjust the free-surface position. First, recall that, as we suppose that the flow is inviscid, the Bernoulli equation allows us to obtain pressure as a function of velocity and height:

$$\frac{p}{\rho} + \frac{1}{2} |\nabla \Phi|^2 + gy = \text{cnst} \quad \text{in } \Omega \quad (3)$$

Mechanical equilibrium of the air-water interface implies that pressure should be equal from both sides of the interface (neglecting surface tension). On the other hand, we suppose that air pressure is constant and equal to  $P_{atm}$ , so that:

$$\frac{1}{2} |\nabla \Phi|^2 + g\eta = \text{cnst} \quad \text{at } \Gamma_{free} \quad (4)$$

where  $\eta(x, z)$  is the surface elevation with respect to the mean elevation  $z = 0$ .

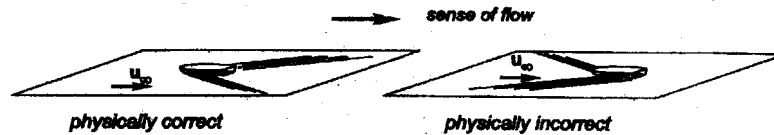


Fig 2: Upwind terms discard non-physical solutions where the wave pattern extends upstream.

However a more detailed analysis shows that the previous problem is ill-posed and this can be seen also through simple symmetry considerations. The previous system of equations is invariant through coordinate inversion  $x \rightarrow -x$ , so that if the body is also symmetric, then for a given solution pair  $\Phi(x, y, z), \eta(x, y)$  to the above equations, then the mirrored pair:  $-\Phi(-x, y, z), \eta(-x, y)$  is also a solution. But it is easy to show that the drag for the mirrored solution is equal but of opposite sign to that one for the original solution, so that two possibilities are open: the solution is symmetric and, then, the drag is null. Or either, the solution to the problem is not unique and an additional condition should be imposed in order to select those solutions that have "physical sense", that is, among other considerations, the drag should be positive and the wave pattern extends from the ship to infinity downstream (see figure).

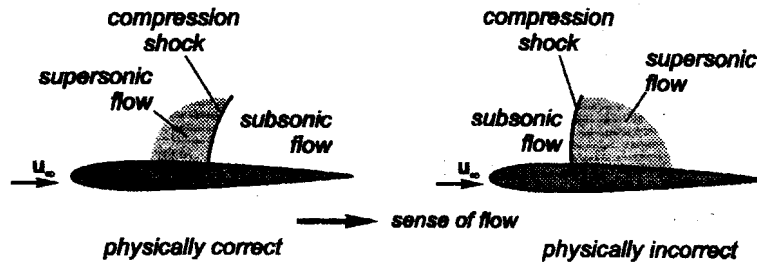


Fig 3: Physical admissible solutions and upwind terms have a close analogy in compressible aerodynamics.

This situation is similar to transonic flow where beyond some critical Mach number, there is a multiplicity of solutions, with "compression" as well as "expansion shock waves". The physically acceptable solution is that one with no expansion shock waves. This is also termed "to satisfy the entropy condition" and is related to the "Second Principle of Thermodynamics", i.e. the generation of entropy should be strictly positive at shocks. Usually, this condition is imposed through the addition of an "upwind", or "numerical diffusion" term. A very common method for the full potential equation is the "upwind in density". In this method the density is evaluated at a point a small distance upwind of the point where velocities are evaluated. This small distance has to be of the same order of the local mesh size.

Inspired in the above mentioned "density upwind technique" for transonic flow, we implemented a scheme which we termed "elevation upwind", where the dynamical condition (4) over the free surface is replaced by:

$$\frac{1}{2}|\nabla\phi|_Q^2 + g\eta_P = \text{cnst} \quad \text{en } \Gamma_{\text{free}} \quad (5)$$

where  $P$  is a point on the surface, slightly upwind from the point where the kinetic energy term is evaluated.

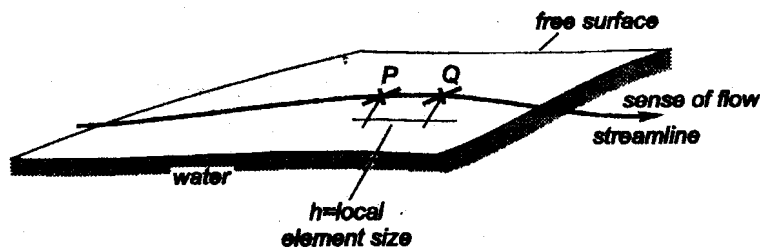


Fig 4: The method of "upwind in elevation"

### THE PANEL METHOD

The underlying panel method is described in detail in a companion paper presented at this same conference [1]. For a given position of the free surface the potential field is obtained from a linear system of the form:

$$\mathbf{A}\boldsymbol{\mu} = \mathbf{C}\boldsymbol{\sigma} \quad (6)$$

where  $\boldsymbol{\mu}$  is the vector of perturbation potentials at the centroids of the panels,  $\boldsymbol{\sigma}$  is the vector of mass fluxes through the panels, and  $\mathbf{A}$  and  $\mathbf{C}$  are full square matrices of interaction coefficients between panels. The vector of fluxes is known from the unperturbed solution (usually a constant velocity flow  $\mathbf{u} = U_{\infty}$ ) and then we have just to solve (6) for the potential vector. Now if the surface is free to adjust itself under the gravity field, then there is an additional set of unknowns, that is the elevations of the nodes on the free surface  $\boldsymbol{\eta}$ . But the interaction coefficients depend on the geometry of the panels, so that the previous system should be rewritten as:

$$\mathbf{A}(\boldsymbol{\eta})\boldsymbol{\mu} = \mathbf{C}(\boldsymbol{\eta})\boldsymbol{\sigma}(\boldsymbol{\eta}) \quad (7)$$

and we have to add the dynamical conditions coming from the upwinded Bernoulli equations (5), which, in discrete form are:

$$\mathbf{R}(\boldsymbol{\eta}, \boldsymbol{\mu}) = 0 \quad (8)$$

Now, equations (7) and (8) are a non-linear system on the pair  $\{\boldsymbol{\mu}, \boldsymbol{\eta}\}$  to be solved with an appropriated method. We propose in the following section a Newton-Raphson based technique.

### THE "DISCRETE" NEWTON-RAPHSON TECHNIQUE

Since equation (7) is linear in  $\boldsymbol{\mu}$ , a simple iterative method based in fixed-point iteration should be the following.

- 1) Choose an initial elevation field:  $\boldsymbol{\eta}^0$ ,  $n \leftarrow 0$
- 2) Compute the potential field  $\boldsymbol{\phi}^n$  from:

$$\mathbf{A}(\boldsymbol{\eta}^n)\boldsymbol{\phi}^n = \mathbf{C}(\boldsymbol{\eta}^n)\boldsymbol{\sigma}(\boldsymbol{\eta}^n) \quad (9)$$

- 3) Compute the new position of the free surface by solving for  $\boldsymbol{\eta}^{n+1}$  from:

$$\mathbf{F}(\boldsymbol{\eta}^{n+1}, \boldsymbol{\phi}^n) = 0 \quad (10)$$

- 4) If not converged:  $n \leftarrow n + 1$ , go to 2)

This strategy is simple and involves only minor modifications to the standard panel code, but it exhibits very low rates of convergence even for very small elevations, in which case the system

is almost linear. We propose then to resort to a Newton-Raphson based algorithm. Now, the computation of the increments  $\{\Delta\mu^{n+1}, \Delta\eta^{n+1}\}$  should be obtained from an equation like:

$$\begin{bmatrix} \mathbf{A} & (\partial\mathbf{A}/\partial\eta)\mu \\ (\partial\mathbf{R}/\partial\mu) & (\partial\mathbf{R}/\partial\eta) \end{bmatrix}^n \begin{bmatrix} \Delta\mu^{n+1} \\ \Delta\eta^{n+1} \end{bmatrix} = - \begin{bmatrix} \mathbf{A}(\eta)\mu - \mathbf{C}(\eta)\sigma(\eta) \\ \mathbf{R}(\eta, \mu) \end{bmatrix}^n \quad (11)$$

Another possibility is to propose a Newton-Raphson scheme for the “continuum equations” and then to discretize that system. The resulting scheme is different from the previous one (since the discretization and Newton-Raphson solution don’t commute) and has some advantages. Firstly, the formulation is by far much more simple as we will see later and, secondly, the number of unknowns in system (11) is  $2N_{fs} + N_{ship}$  where  $N_{fs}$  is the number of panels in the free surface and  $N_{ship}$  the number of panels on the ship skin, whereas in the proposed formulation the number of unknowns is simply  $N_{fs} + N_{ship}$ . Since in general,  $N_{fs} > N_{ship}$  and in a lot of situations  $N_{fs} \gg N_{ship}$ , this is a significant save in computing resources.

### THE “CONTINUUM” NEWTON-RAPHSON METHOD

Suppose now that we have approximated values for the perturbation potential  $\phi$  (defined by  $\Phi = \mathbf{u}_\infty \cdot \mathbf{x} + \phi$ ) and elevation fields  $(\phi, \eta)^n$ . As usual, we will consider that the next iteration values  $(\phi, \eta)^{n+1}$  will be close to  $(\phi, \eta)^n$  and this a first order expansion is performed in the increments:

$$\begin{aligned} \phi' &= \phi^{n+1} - \phi^n \\ \eta' &= \eta^{n+1} - \eta^n \end{aligned} \quad (12)$$

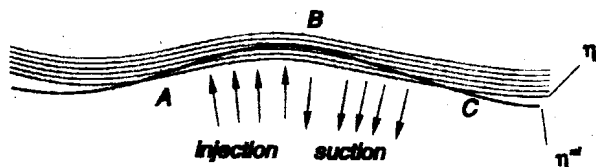


Fig 5: The “transpiration flux” method

The linearized (not upwinded) Bernoulli equation is:

$$\mathbf{u} \cdot \nabla \phi' + g\eta' = \frac{1}{2}(u_\infty^2 - |\nabla \phi^n|^2) - g\eta^n = R_{\text{Bernoulli}}^n \quad (13)$$

On the other hand, we have to find a linearized expression for the potential increment  $\phi'$  when a small perturbation in the free surface  $\eta'$  is produced. As both  $\phi^n$  and  $\phi^{n+1}$  should be harmonic and with homogeneous boundary conditions at the ship and infinity boundaries, and these boundaries don’t change with the perturbation on the free surface, it is clear that this equations apply also for the increment  $\phi'$ . The only thing that changes is the free surface position, and we should be able to put this as a source term in the boundary condition for the increment. This can actually be done through a “transpiration flux” technique, which is a perturbation expansion technique [3] and can be easily understood from figure 5. Let  $\mathbf{u}^n$  be the velocity at the  $n$ -th iteration corresponding to a position of the free surface given by  $\eta^n$ . Then, a small perturbation in the position of the free surface  $\eta'$  can be simulated by adding “blowing” at those points where the new position  $\eta^{n+1} = \eta^n + \eta'$  tends to separate from the old position  $\eta^n$ , whereas “suction” should be added at those points where

$\eta^{n+1}$  tends to approach  $\eta^n$ . The detailed perturbation expansion shows that the transpiration flux should be:  $\mathbf{u}^n \cdot \nabla \eta'$ , and then the complete problem for  $\eta'$  is:

$$\begin{aligned} \Delta \phi' &= 0, & \text{en } \Omega \\ \frac{\partial \phi'}{\partial n} &= 0, & \text{en } \Gamma_{\text{ship}} \\ \frac{\partial \phi'}{\partial n} &= \mathbf{u}^n \cdot \nabla \eta', & \text{en } \Gamma_{\text{ship}} \end{aligned} \quad (14.1, 2, 3)$$

Solving for  $\eta'$  from (13) and replacing in (14.3), we arrive to a boundary condition for  $\phi'$ :

$$\frac{\partial \phi'}{\partial n} + \left( \frac{1}{g} (\mathbf{u}^n \cdot \nabla) (\mathbf{u}^n \cdot \nabla) \phi' \right)_{\text{upw}} = \frac{1}{g} (\mathbf{u}^n \cdot \nabla) R_{\text{Bernoulli}} \quad (15)$$

This is the upwinded version, which is indicated by the subindex in the second term of the left hand side, which means that the given quantity should be evaluated a little distance upwind from the current location where the other terms are being evaluated.

### NUMERICAL IMPLEMENTATION OF THE FREE SURFACE BOUNDARY CONDITION

Recall that  $\sigma$  in (6) stands for the mass fluxes coming from the non-perturbed flow. For the incremental problem, the applied fluxes are the right hand side of (15) minus the second term of the left hand side. Thus the discrete equations are:

$$\mathbf{A} \boldsymbol{\mu}' = \mathbf{C} (-\mathbf{D} \boldsymbol{\mu}' + \mathbf{r}) \quad (16)$$

where  $\mathbf{D}$  is the discrete version of the upwinded second order derivative operator along the streamline (also termed "diffusive operator"), and  $\mathbf{r}$  the discrete residual of the Bernoulli equation. To solve for  $\boldsymbol{\mu}$ , one has to solve a linear system with coefficient matrix  $\mathbf{A} + \mathbf{CD}$ . Matrix  $\mathbf{D}$  is scaled by  $K = U_{\infty}^2/g \propto Fr^{-2}$  (assuming a fixed ship length  $L$ ), where  $Fr = U_{\infty}/\sqrt{gL}$  is the non-dimensional Froude number. It can be shown that as  $Fr$  is increased, the  $\mathbf{CD}$  term tends to destabilize the problem. The condition number of the system highly depends on the amount of numerical diffusion, i.e. to the length scale used in the upwinding.

To set up a numerical approximation for the diffusive operator is not straightforward. Firstly, if one tries to set up a FEM approximation over the underlying 2D FEM mesh that results to restrict the panel mesh to the free surface, then one has the difficulty that the potentials given by the panel method should be considered at the center of the panel, so that prior to any FEM manipulation, a conversion from elemental to nodal values should be performed, what is an additional source of error. Secondly, one can't integrate by parts the streamlined second derivative operator since:

$$\begin{aligned} \int_{\Gamma_{\text{free}}} \psi (\mathbf{u}^n \cdot \nabla) (\mathbf{u}^n \cdot \nabla) \phi' d\Gamma &= - \int_{\Gamma_{\text{free}}} (\mathbf{u}^n \cdot \nabla \psi) (\mathbf{u}^n \cdot \nabla \phi') d\Gamma - \\ &- \int_{\Gamma_{\text{free}}} \psi (\nabla \cdot \mathbf{u}) (\mathbf{u}^n \cdot \nabla \phi') d\Gamma + \text{boundary term} \end{aligned} \quad (17)$$

where  $\psi$  is any weight function. One is tempted to discard the  $\nabla \cdot \mathbf{u}$  term due to incompressibility, but recall that the integral is not over a volume but over a surface and then the divergence term has to be interpreted as its 2D projection  $(\nabla \cdot \mathbf{u})_{\Gamma} = (\partial u/\partial x) + (\partial v/\partial y) = -(\partial w/\partial z)$  which is not necessarily zero. The situation is further complicated since the boundary term is in fact, a line integral over the intersection between ship-hull and free surface and has not an evident physical interpretation. Third and last, the upwinded version should involve third order derivatives, what precludes the use of the standard (SUPG for instance) upwind techniques.

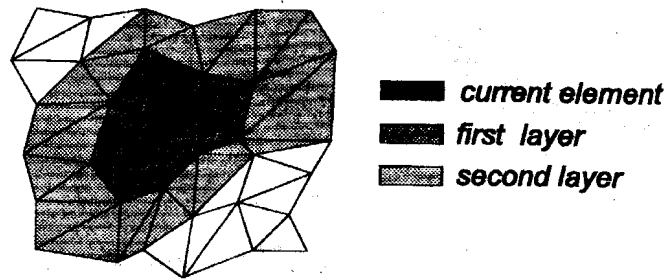


Fig 6: Layers of panels around the current panel.

We, then, resorted to a “mesh-less approximation”, but taking profit of the underlying panel mesh. Recall that mesh-less approximations to a given differential operator consist in selecting a “cloud” of neighboring points and least-squares fitting the values at these points by a (high order enough) polynomial. Then, the differential operator is approximated as the operator applied to the polynomial. A key point of the method is the selection of the cloud and weight for each point of the cloud. The usual method in the literature is to use weights which depend on the distance between the nodes and with compact support, i.e. they are null for those nodes outside a circle with some specified radius. The cloud is simply those nodes with a non null weight. In this work, we used the underlying panel mesh to select the cloud and the weights, based in the distance (in the sense of “graphs”) from the current point to the potential candidates to be incorporated in the cloud. Consider for instance, the dark shadowed panel in figure 6. The panels are considered nodes in a non-oriented graph, and two panels are considered linked if they have at least one node in common. Then we mark those panels linked to the current panel as being “on its first layer”. Those panels linked to those on the first layer, but not pertaining to it, are marked as the second layer, and so on. The cloud is selected as those panels pertaining to, at most, the  $n_{lay}$ -th layer. The number of layers should be in accordance with the order  $p$  of the polynomial to be fitted, and this, in turn, should be in accordance with the order of the differential operator  $l$ . The order of the approximation will be  $O(h^o)$  with  $o = p - l + 1$ , so that we need  $p \geq l$  in order to have a convergent approximation. On the other hand, if we think at the one-dimensional case, then we need at least  $p + 1$  points in order to fit a polynomial of order  $p$ . But the number of points in the stencil in the 1D case is  $2n_{lay} + 1$ , so that we need  $2n_{lay} \geq p$ .

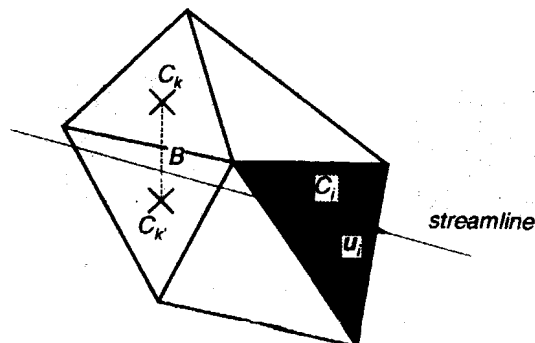


Fig 7: The discrete setup for the upwind term.

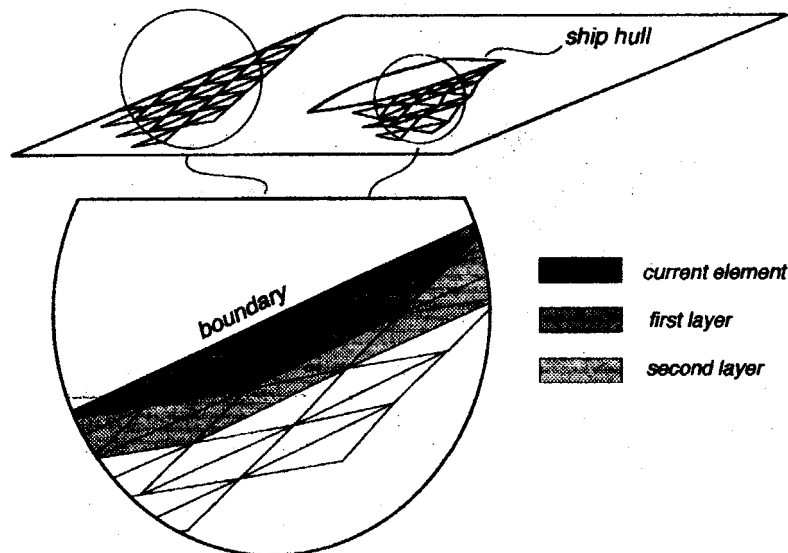


Fig 8: The number of layers in the stencil must be increased for the panels at the boundaries, i.e. those in contact with the ship hull as well as the infinite boundary.

In our case, we approximated the upwind streamlined second order derivative operator in terms of the centered one by (see figure 7):

$$(\mathcal{D}_{\text{upw}}\phi)_i = (1 - \alpha)(\mathcal{D}\phi)_i + \alpha[\rho(\mathcal{D}\phi)_k + (1 - \rho)(\mathcal{D}\phi)_{k'}] \quad (17)$$

Where  $k, k'$  are those panels pertaining to the first layer such that the streamline that passes through the center  $C_i$  of panel  $i$  traverses the segment  $C_k C_{k'}$  that joins their centers. The term in brackets represents the value of  $(\mathcal{D}\phi)$  at the point  $B$  where the streamline intersects this segment, so that  $\rho = BC_{k'}/C_k C_{k'}$ . On the other hand,  $0 \leq \alpha \leq 1$  controls the amount of numerical diffusion,  $\alpha = 0$  implies no upwind, and  $\alpha = 1$  implies "full upwind":  $(\mathcal{D}_{\text{upw}}\phi)_i = (\mathcal{D}\phi)_B$ . The centered operator corresponds then to  $l = 2$ , and then we choose  $p = 2$  and  $n_{\text{lay}} = 1$ . This will give an  $O(h)$  approximation according to the analysis given above.

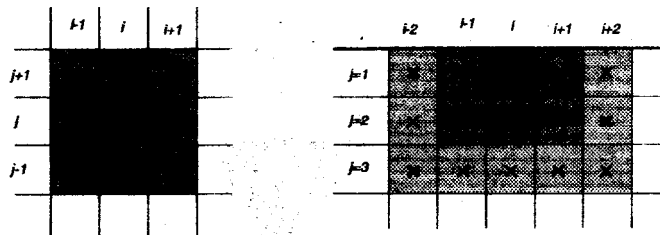


Fig 9: Stencils for the Laplace operator on a homogeneous square mesh. Right: interior panel (see coefficients in Table I). Left: Boundary panel (see coefficients in Table II).

A special treatment has to be given to those panels that are on the boundary- 8. We mean by this, those panels for which an inner layer (layer number strictly lower than  $n_{\text{lay}}$ ) is in contact



Table I: Coefficients  $C_{ij}$  for the Laplace operator on a square mesh for an interior panel

	$i-1$	$i$	$i+1$
$j+1$	$\frac{4}{9}$	$\frac{1}{9}$	$\frac{4}{9}$
$j$	$\frac{1}{9}$	$-\frac{20}{9}$	$\frac{1}{9}$
$j-1$	$\frac{4}{9}$	$\frac{1}{9}$	$\frac{4}{9}$

Table II: Coefficients  $C_{ij}$  for the Laplace operator on a square mesh for a boundary panel

	$i-2$	$i-1$	$i$	$i+1$	$i+2$
$j=1$	0.07404	0.21651	0.41890	0.21651	0.07404
$j=2$	-0.00793	-0.60317	-0.77779	-0.60317	-0.00793
$j=3$	0.23492	0.18254	0.16508	0.18254	0.23492

with the boundary. This elements risk to have a singular matrix at the moment of solving the least squares system for the polynomial fitting. One solution is to add elements from the side of the panel opposite to that one which is in contact with the boundary. This can be thought as taking "one-sided" stencils in a finite difference context. In our case, we took simply  $n_{lay} = 2$  for those panels in contact with the boundary.

The weights were taken as  $w_j = \tilde{w}^d$ , where  $d$  is the topological distance from the current panel to the  $j$ -th panel, what is the same to the number of the layer to which the  $j$  panel pertains and  $\tilde{w} \ll 1$ . This means that the weight of those panels on the  $l+1$  layer are equal and  $\tilde{w}$  times that ones on the previous  $l$  layer. Setting  $\tilde{w}$  low tends to give a stencil more concentrated to the center. But setting it too low can give a stencil too sensible to the position of the nodes in some configurations. We have set  $\tilde{w}=0.1$  in the examples. As an example, we show in Tables I and II, the stencils obtained for the Laplace operator on a homogeneous mesh of square panels of mesh spacing  $h$ , for interior and boundary panels (see figure 9), i.e. the method gives an approximation of the form:

$$\left(\frac{\partial^2}{\partial x^2} + \frac{\partial^2}{\partial y^2}\right)\phi = \sum_{i,j} C_{ij} \phi_{ij} + O(h) \quad (18)$$

and we show in the tables the coefficients  $C_{ij}$  in both cases.

### CONCLUSIONS

The solution of the wave-drag problem in ship hydrodynamics requires the approximation of an upwinded streamlined second order derivative operator. The complexity of the operator in addition to the restrictions of the underlying panel discretization make it difficult the use of standard (i.e. FEM/FDM) discretization techniques. The proposed "mesh-less" approximation has been proved to be an interesting tool since it gives a large freedom in the operator to discretize and the order of approximation. All this in the context of a general, unstructured panel mesh.

**REFERENCES**

- [1] J. D'Elia, M. Storti and S. Idelsohn "A 3D Panel Code for Wave Drag Calculations. Part I: General Formulation and Discretization" to be presented at MECOM'96.
- [2] S. Ohring, "Three Dimensional Ship Wave Generation Using an Efficient Finite Difference Scheme with Double Model Linearization", Journal of Comp. Physics vol 41, 89-114 (1981).
- [3] M. Van Dyke, "Peturbation Methods on Fluid Mechanics", The Parabolic Press, Stanford, (1975)